Powell River Project 2020-2021 Annual Research Report

Assessing Flow-driven Effects on Local and Downstream Water Quality in Central Appalachian Headwater Streams Influenced by Surface Coal Mining

D. McLaughlin[a], S. Schoenholtz[b], C. Zipper[c], B. Heskett[a], M. McMillan[a], A. Timpano[d], S.A. Entrekin[e], E.R. Hotchkiss[f]

[a] Department of Forest Resources and Environmental Conservation, Virginia Tech
[b] Virginia Water Resources Research Center, Virginia Tech
[c] School of Plant and Environmental Sciences, Virginia Tech
[d] Department of Fish and Wildlife Conservation, Virginia Tech
[e] Department of Entomology, Virginia Tech
[f] Department of Biological Sciences, Virginia Tech
*corresponding investigator (mclaugd@vt.edu)

Introduction

Surface coal mining has been a common land use alteration in central Appalachia for a half century. Mining removes vegetation and overlying layers of bedrock to expose buried coal seams. Fractured waste rock produced during this process undergoes accelerated weathering, thereby releasing increased amounts of major ions (e.g., SO_4^{2-}, HCO_3^-, Ca^{2+}, Mg^{2+}) and trace elements (e.g., As, Cd, Cu, Ni, Se, Sr, V, Zn) to headwater streams (Hartman et al. 2005; Pond et al. 2008; Timpano et al. 2015). Alterations to water chemistry, particularly increased salinity, are well-documented (Griffith et al. 2012), along with associated impacts to benthic macroinvertebrates, including loss of sensitive species (Pond 2010) and communities shifted to more-tolerant taxa (Pond et al. 2008; Timpano et al. 2015, 2018). Despite the well-recognized impacts of mining on headwater streams, less is known regarding potential stream recovery, calling for long-term study of both water chemistry and biological conditions. Our ongoing research focuses on such long-term trends and, to date, has found limited declines in SC and associated recovery of macroinvertebrate communities with time since mining (Cianciolo et al., 2020a). However, further study is needed to track potential recovery of both water chemistry and benthic communities, and with expanded focus on: i) streamflow influences on water chemistry; ii) relationships between SC and concentrations of major ions and trace elements; and iii) headwater contributions of such water quality constituents to downstream waters.

Streamflow Effects on Water Chemistry

Dissolved ion concentrations naturally vary as a result of streamflow variation, often exhibiting either enrichment or dilution with increased flow (Griffith et al. 2012; Clark et al. 2016). Indeed, with PRP support, we have documented inverse relationships between SC and water level (as an indicator of flow variation) at our study streams, indicating dilution under high flow conditions. Consequently, long-term trend analysis to assess water chemistry recovery is complicated by this additional driver of SC, requiring continued data collection and statistical methods to indirectly account for it with seasonal-based approaches (e.g., seasonal Kendall analysis; Hirsch at al. 1982).

Major Ions and Trace Elements

Although SC is often used as an indicator of the potential for mining-influenced streamwater to affect aquatic life (e.g., Pond et al. 2008; USEPA 2011; Timpano et al. 2018), waters with a given SC can vary in concentrations of specific major ions and trace elements. Toxicity of high-salinity waters is dependent upon the major ions present (e.g., Soucek et al. 2018; Mount et al. 2019), and our preliminary data, with PRP support, indicate that major-ion composition is not constant across the gradient of SC (e.g., sulfate is a more dominant anion at higher SC). Although this preliminary finding is consistent with results of mine-spoil leachate studies (Clark et al. 2018), major-ion relationships with SC in mining-influenced Appalachian waters have not been thoroughly assessed. Further, trace element concentrations in these systems, excepting selenium (Se), have been scarcely explored, although multiple trace elements that differ in bioaccumulation potential and associated toxicity are present in Appalachian mine-spoil leachates (Clark et al. 2018). To that end, we have documented bioaccumulation of several trace elements in a subset of our mining-influenced streams (Whitmore et al. 2021), with a major focus on Se (Whitmore et al. 2018; Cianciolo et al. 2020b). Given such bioaccumulation potential, both locally and in downstream waters, there is a need to more thoroughly quantify trace elements in Appalachian headwater streams influenced by surface coal mining. With PRP support, we have accumulated hundreds of water quality measurements from our study streams over multiple years. These data provide the opportunity to assess if major-ion and specific trace element concentrations in mining-influenced waters vary predictably with SC and flow conditions.

Downstream Loads

Major ions and trace elements in mining-influenced headwater streams can have important consequences for downstream waters (Johnson et al. 2019). In central Appalachia, however, there has been limited research to understand changes in loads (or mass contributions) of water chemistry constituents (e.g., major ions, trace elements) to downstream waters. Relationships between SC and constituent concentrations, together with continued data collection for SC, water level and flow data, can yield such downstream loads and inform monitoring approaches relevant to the total maximum daily load (TMDL) framework (CWA §303(d)(1)(C)).

Project Objectives

With PRP support, our interdisciplinary research group continues to assess local and downstream water quality consequences of surface mining as part of our long-term monitoring of 24 central Appalachian headwater streams since 2011. [Note that we recently terminated measurements in one study stream due to hydrologic alterations from beaver dams.] This study is unique in its length of time as well as its breadth of data collection. Specifically, efforts have included 30-minute SC measurements and biannual sampling of benthic macroinvertebrates and water chemistry. We have also worked in subsets of these 24 study streams to advance scientific understanding of i) surface mining effects on trace element bioaccumulation (Cianciolo et al. 2020a; Whitmore et al. 2018) and selected carbon dynamics (VanderVorste et al. 2019), ii) seasonal changes and increased accuracy for quantification of benthic macroinvertebrate communities (Boehme et al. 2016; Pence 2019), and iii) stream geomorphology (Drover 2018). In this PRP-supported project, we continued this collective body of work by building upon our long-term dataset for water chemistry and macroinvertebrate community structure, comprising

data necessary to assess potential stream recovery after mining. Further, we continued water level monitoring and flow measurements to understand flow-driven variation in water chemistry. Last, we initiated new data analysis efforts to develop relationships between SC and major ions and trace elements, allowing predictions of their concentrations in our headwater streams and, with flow data, novel estimates of their loads to downstream waters. Specific objectives included:

1. Expand temporal scope for continuous SC monitoring and seasonal sampling for benthic macroinvertebrates and synoptic water chemistry in 23 central Appalachian headwater streams initiated in 2011.
2. Assess water level- and flow-driven variation in water chemistry to inform analyses of long-term trends in SC, dissolved major ions, and trace elements.
3. Develop predictive relationships between SC and major ion and trace element concentrations.
4. Quantify mass fluxes of dissolved major ions and trace elements to downstream waters.

Methods

Data Collection

Water Level and Streamflow

We installed HOBO U20 water level dataloggers (6 matched by VWRRC, 8 purchased with previous PRP support) across 14 of our 23 study streams to measure stream stage. Dataloggers were placed inside screened wells within each stream and record stage every 30 minutes. Additional dataloggers were installed in streamside areas to collect and account for local barometric pressure variation. At a subset of streams (2 reference, 4 mined) we measured flow during site visits with the attempt to capture a range in flow magnitudes. To do so, we used salt tracer additions (Gooseff et al. 2003) and measured response in SC levels (instrumentation described in *Water Chemistry* section below). Using the known volume and concentration of the salt solution, and stream background SC, stream discharge was estimated from the following equation:

$$Q = \frac{V}{k\Delta t \sum_{i=0}^{n}[\mathrm{EC(t)} - EC_{bg}]} \quad \text{(Eq 1)}$$

where Q is stream discharge (m^3/s), V is the known volume of the injection slug (m^3), k is the calibration constant, EC(t) is the electrical conductivity at time t, and EC_{bg} is background conductivity of the stream (Moore, 2005). With matching student-support funding, we will continue flow measurements for the same six streams so that a stage-flow relationship (i.e., rating curve) can be developed for each stream, yielding sub-daily flow estimates from 30-minute stage data.

Water Chemistry

We continued our long-term monitoring of selected water quality parameters in 23 study streams initiated in 2011. In situ SC data are recorded every 30 minutes using automated dataloggers (HOBO Freshwater Conductivity Data Logger, model U24-001, Onset Computer Corp., Bourne, Massachusetts) already installed within each stream. Grab samples of streamwater were collected in spring 2021 to assess major ion and trace element concentrations. Vertically mixed water was

collected and immediately filtered through a 0.45-µm pore polyvinylidene fluoride filter into pre-labeled sterile polyethylene sample bags. The cation sample was preserved to pH < 2 by adding approximately 0.5% (v/v) of a solution of 1+1 concentrated ultrapure nitric acid and deionized water (UESPA 1996). Samples were stored at 4° C until analysis. Samples were analyzed for total dissolved solids (TDS) by evaporating streamwater to constant weight in a drying oven at 180° C (USEPA 1971). Total Alkalinity was measured by titration of stream water samples with a prepared standard acid (0.02N HCl) using a potentiometric auto-titrator (TitraLab 865, Radiometer Analytical, Lyon, France) (APHA 2005). Calculations of HCO_3^- were made from Total Alkalinity and pH measurements (APHA 2005). Samples were analyzed for major cations/trace elements and SO_4^{2-} by ICP-MS (Thermo iCAP-RQ) (UESPA 1996) and ion chromatograph (Dionex ICS 3000), respectively.

Benthic Macroinvertebrates

As has been done since 2011, benthic macroinvertebrates were sampled in spring 2021 in 23 study streams using the semi-quantitative, single habitat (riffle-run) method established by the Virginia Department of Environmental Quality (VDEQ 2008), which is adapted from U.S. EPA Rapid Bioassessment Protocols (RBP; Barbour et al. 1999) and comparable to the method used by West Virginia Department of Environmental Protection (WVDEP 2015). Using a 0.3-m D-frame kicknet with 500-µm mesh, a single composite sample (approximately 2 m^2) composed of six approximately 1×0.3-m kicks was collected from separate riffles along a 100-m reach upstream of the SC datalogger. Samples were preserved in 95% ethanol and returned to the lab for sorting and identification. Macroinvertebrate samples were sub-sampled randomly to obtain a 200 (±10%) organism count following VDEQ biomonitoring protocols (VDEQ 2008). Specimens were identified to genus using standard keys (Merritt et al. 2008), except individuals in family Chironomidae and subclass Oligochaeta, which were identified at those levels.

Data Analysis

Trend Analyses and Flow Controls

Water chemistry data (seasonal and in situ SC) and macroinvertebrate metrics support continued trend analysis to assess changes that may have occurred since 2011. We also assessed site-specific relationships between SC and water level data (as a surrogate for flow) to describe solute enrichment or dilution with increased flow. These relationships will assess flow controls on water chemistry variation, thereby allowing us to incorporate this natural driver in future long-term trend analyses using such statistical approaches as seasonal Kendall analysis (Hirsch at al. 1982) and/or our previous seasonal sinusoidal models (Timpano et al. 2018).

SC-Concentration Relationships

Database and Processing

Using our database for concentrations of major ions (Ca^{2+}, Mg, $^{2+}$ Na^+, K^+, SO_4^{2-}, Cl^-, HCO_3^- + CO_3^{2-}) since 2011 and for dissolved trace elements (including Al, Cu, Fe, Mn, Ni, Se, Zn) since 2013 (Table 1), we assessed each constituent's relationship with coincident SC measurements via several model forms. Prior to modeling, several data-processing steps were conducted.

Table 1. Numbers of samples by season and year.

Quarter	2011	2012	2013	2014	2015	2016	2017	2018	2019	2020	2021	Total
Spring	17	23	23	23	0	23	14	20	23	0	22	188
Fall	23	23	22	0	23	22	22	23	23	22	0	203

Note: Spring samples were obtained between 3/22 and 6/7; fall samples were obtained between 10/4 and 11/17.

Minimum reporting level (MRL) and minimum detection levels (MDL) varied among laboratories, and some trace-element concentrations were available only for some sampling events. For most years and seasons, trace-element concentrations detected as ≤MDL levels or as >MDL but ≤MRL were analyzed as the instrument read-out values, reasoning that these values contain usable information about relative concentration magnitudes. Because those values were not available for year 2019 samples, year 2019 data for trace elements with multiple <MRL values were excluded from the analyses. Most trace elements with >50% of observations identified as <MRL/<MDL were excluded from the analyses. Copper and Se, however, were included despite high fractions of <MRL/<MDL observations because of their environmental significance.

Mole fractions were calculated for anions and cations separately. For each major ion variable (including CO_3^{2-} and HCO_3^- combined) for each observation, the mole fraction for each major-ion variable was calculated as:

$$\text{Mole Fraction} = Y_{i\text{-}m} / \sum Y_m \quad \text{(Eq. 2)}$$

Where $Y_{i\text{-}m}$ = the i^{th} constituent's concentration expressed as mmol/L, and $\sum Y_m$ = the sum of molar concentrations for either all major anions or all cations as appropriate to the constituent.

Last, distributions of measured values for each constituent as measured and as Ln-transformed were inspected to identify more-normal distributions for model application (Helsel and Hersh, 2002). If a constituent with zero or negative machine read-out values for <MRL/<MDL observations required Ln transformation, a constant was added to all raw values for that constituent prior to Ln transformation. The constant was selected as the lowest-magnitude factor of 10 that eliminated nominally negative or zero values.

Model Forms

Three primary model forms were used for analysis: i) multiple regression models for all major ions, pH, and ion ratios; ii) mixed effects models with SC as the fixed effect and sampling event as a random effect for all water quality variables (including trace elements); and iii) site mean model using site mean values (for SC and water quality variable) for only trace elements. Reasoning for model selection is discussed below. All modeling activity was conducted using JMP Pro v. 15 software (SAS Institute, Cary NC).

Multiple Regression Model:

$$Y^{\ddagger} = f\,[SC^{\ddagger}, \text{year}, \text{season}] \quad \text{(Eq. 3)}$$

where $Y^{\ddagger}$ = the water quality variable expressed as measured values or the Ln-transformation of measured values, and $SC^{\ddagger}$ = SC expressed either as-measured or as an Ln transformation.

Modeling was conducted as a full factorial with seven terms initially including the three-factor interaction and all three two-factor interactions. For these analyses, year was converted to a 2-digit numeric identifier (2011 becomes year 11, etc.) and season was converted to a numeric term (0 = spring, 1 = fall). Backwards-selection procedures were used to refine the regression model, deleting non-significant ($p>0.05$) interactions. The three-factor interaction term was always non-significant. It was deleted first, then the model was re-run sequentially, deleting additional non-significant interaction terms in inverse relationship to their p-values for the sequential model runs. The final model included all three primary terms and any interactions that retained statistical significance at $p<0.05$. In addition to the final model form, variable importance factors were tallied as total effects assuming independent uniform inputs.
After noting the predominant influence of SC on modeled concentrations as indicated by variable importance factors, model results for each major ion and pH were plotted as a function of SC using the mid-point of the year (16) and season (0.5) variables. Multiple regression modeling was not applied to trace elements because most trace elements included <MRL observations with machine read-out values as proxy for actual concentrations. Although we expect these values to reflect relative magnitudes of concentrations measured during that analysis run, there is no reason to expect <MRL/<MDL threshold values as generated by different instruments and laboratories to be comparable across analytical runs.

Mixed-Effects Model:

$$Y^{\ddagger} = f\,[SC^{\ddagger}, \text{sample event (random)}] \quad \text{(Eq. 4)}$$

Where $Y^{\ddagger}$ = the water quality variable, expressed either as measured or as an Ln-transformation of measured values, $SC^{\ddagger}$ = SC as a fixed effect (as-measured or as an Ln transform), and sampling event as a random variable. This model form provided a more direct and interpretable relationship with SC. Mixed effects models were also applied for trace elements because this model form analyzes data within each sampling event separately and then combines those sampling-event results to produce an overall result, with no comparison of variable magnitudes among sampling events. Hence, this form is appropriate for the trace-element data structures that combine sub-MRL and measured values.

Site Means Model:

$$Y^{\ddagger}_{SM} = f\,[\,SC^{\ddagger}_{SM})] \quad \text{(Eq. 5)}$$

$Y^{\ddagger}_{SM}$ = the site-mean trace-element concentration either as-measured or Ln-transformation of the measured values, and $SC^{\ddagger}_{SM}$ = the site-mean SC, either as calculated from measured values or as the Ln transform. Because of known seasonal effects (Timpano et al. 2018b), stream means were calculated by first calculating seasonal means for each variable at each site, and then calculating the stream mean from the two seasonal mean values. This additional modeling step was conducted only for trace elements to further assess their relationship with SC given that multiple regression models were not applied.

Downstream Loads

Developed SC-constituent relationships (above) and 30-minute SC data will enable estimates of 30-minute concentrations for major ions and trace elements. With future flow measurements (and developed stage-flow rating curves), we will couple these estimated concentrations with flow estimate time series to yield sub-daily mass fluxes (or loads) to downstream waters. As such, data collected in this project and continued work using established monitoring sites will assess daily mass loading rates and how they vary across sites, seasons, and flow conditions.

Results and Discussion

Streamflow and Water Chemistry

At each of our 23 stream sites, we expanded our continuous 30-minute SC and added water level monitoring from Fall 2019 through summer of 2021 (Figure 1). We observed inverse relationships between SC and water level at all study streams, indicating dilution under high flow conditions (Figure 2). However, the magnitude of this flow-induced dilution was greater in salinized streams (e.g., from ca. 35 to 20 µS/cm in the reference stream in Figure 2A vs.700 to 250 µS/cm in Figure 2B).

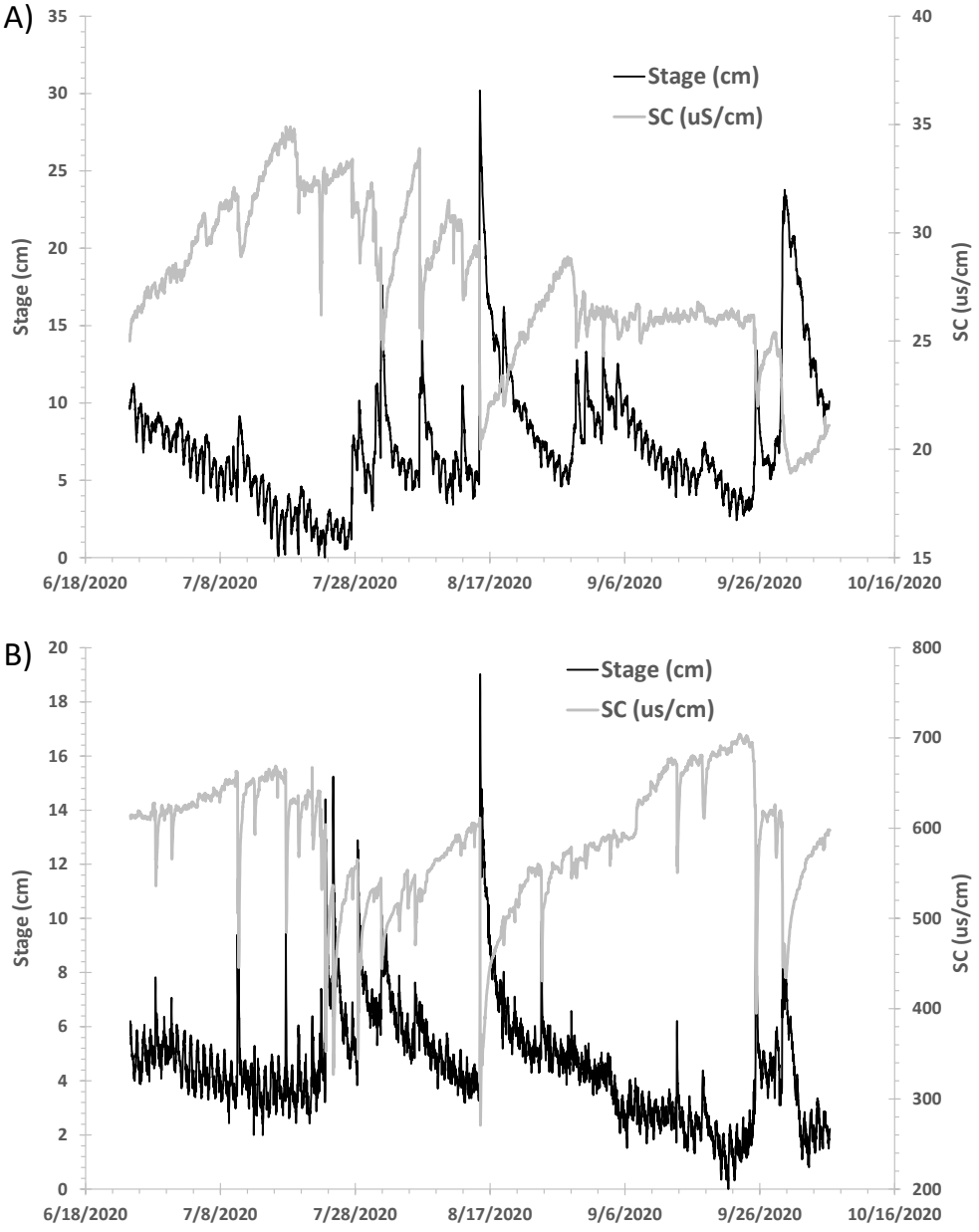

Figure 1: Time series of stage and specific conductance (SC) at a reference stream (A) and a salinized stream (B).

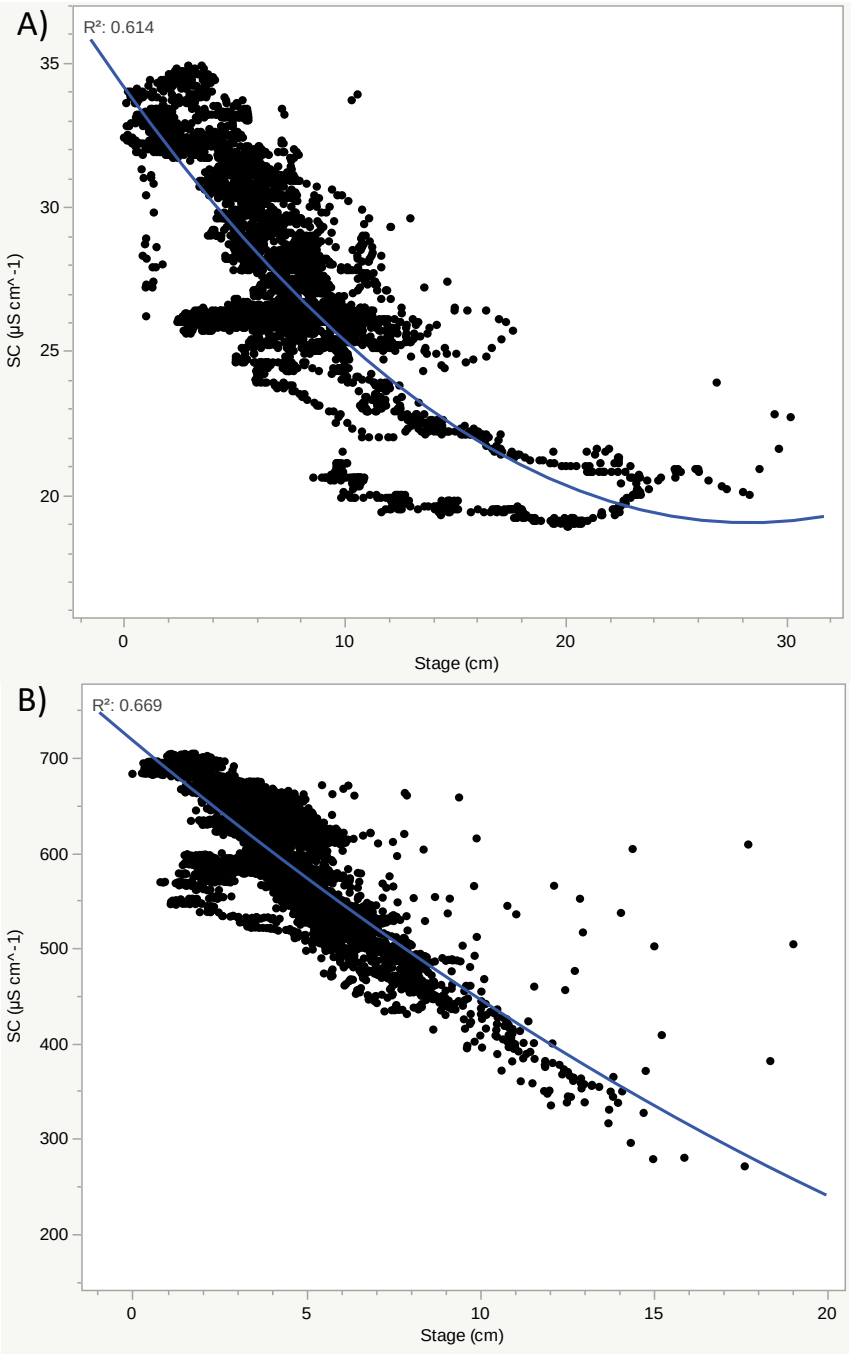

Figure 2: Specific conductance (SC) versus water level in a reference stream (A) and a salinized stream (B) from fall 2019 to summer 2021.

Flow measurements (via salt injections) at six study streams were conducted for development of stage-flow rating curves. Salt injections resulted in a 25 – 75% increase in salinity from background to produce a "wave" large enough to derive an estimate of stream flow (Figure 3). Baseflow flows were documented in the first round and ranged from 0.7 l/s to 67 l/s across the

sampled streams (Table 2). To produce an accurate rating curve, future salt tracer additions will be conducted across a range of flows using established instrumentation and match student-support funding. Once an accurate rating curve is developed for each of the six study streams, sub-daily flow estimates can be calculated, enabling load estimates for different water chemistry variables using the SC-concentration relationships developed below.

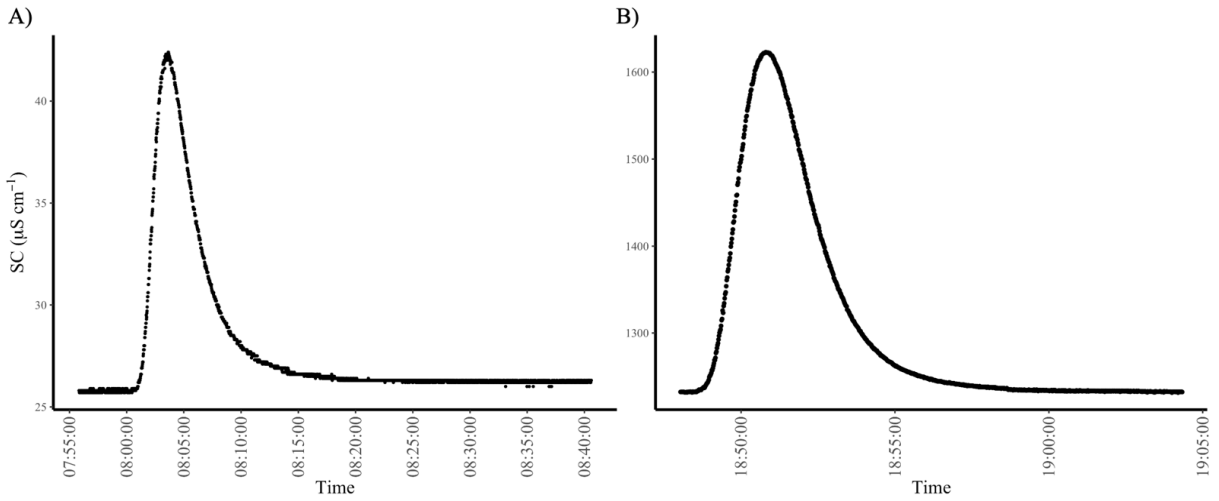

Figure 3: Recorded SC wave created from salt slug additions to a reference stream (A) and a salinized stream (B). The area under the curve is used to calculate stream flow at a given point in time and water level.

Table 2: Initial salt tracer results at six streams. Amount of salt (NaCl) used, mixing length, and time for tracer test to complete varied by watershed area and background SC concentration. *We conducted another round of flow measurement at these streams, and data currently are being processed to determine flows.

Site	Background SC	Watershed area (km^3)	% Watershed Mined	NaCl (g)	Slug Time (mm:ss)	Mixing Length (m)	Water level (cm)	Flow (l/s)
EAS	26	2.2	0	20	25:00	41	13.9	0.7
HCN	72	6.0	0	100	20:00	70	9.7	8
CRA	424	9.8	NA	200	22:50	85	11.7	67
SPC	506	6.9	2.2	250	45:00	100	19.7	12
MIL	655	2.7	55.3	300	22:00	40	17.7	9
LLW	1205	2.0	27.2	400	21:30	48	11.7	17

SC-Concentration Relationships

Twenty-six water-quality variables were analyzed for relationships with SC, including pH, seven major ion concentrations, seven major-ion mole fractions, and eleven trace elements (Table 3). Few of the models produced residuals that conformed with normal distributions as indicated by Anderson-Darling statistics. All variables produced residual distributions with a somewhat normal appearance and lacking extreme outliers. Nonetheless, p-values generated by the models should be considered as nominal indicators and not interpreted in a strict statistical sense; but the very low p-values generated by most models indicate high levels of statistical confidence.

Table 3. Numbers of observations (total and <MRL), mean, minimum, and maximum values for SC, pH, major ions, and trace elements analyzed; and the variable transformation applied for analysis.

Site Type	- - - - - Mining Influenced Sites - - - -					- - - - - - Reference Sites - - - - - -					Analysis
	N	<MRL	Mean	Min	Max	N	<MRL	Mean	Min	Max	
SC (µS/cm)	305	0	766	114	1979	86	0	69	20	196	Ln (SC)
pH (s.u.)	284	0	7.95	6.94	8.82	81	0	7.41	5.78	8.54	Ln (pH)
Major Ions (mg/L)											
Cl^-	291	0	5	0.3	32	81	0	2	0.2	9	Ln (Cl^-)
$SO4^{2-}$	292	0	309	29	1031	80	0	10	2	21	Ln (SO_4^{2-})
CO_3^{2-} + HCO_3^-	292	0	127	19	306	81	0	26	6	109	Ln (CO_3^{2-} + HCO_3^-)
Na^+	294	0	20	4	105	82	0	3	0.5	15	Ln (Na^+)
Mg^{2+}	294	0	50	4	196	82	0	2	1	7	Ln (Mg^{2+})
K^+	294	0	4	1.2	16	82	0	1	0.3	2	Ln (K^+)
Ca^{2+}	294	0	75	10	209	82	0	6	2	21	Ln (Ca^{2+})
Trace Elements (µg/L) †											
Al	218	43	9.4	<1.48	54.0	62	13	7.6	1.3	26.8	Ln(Al)
Ba	149	63	46.2	<21.89	158.7	43	19	39.5	<9.94	179.1	Ln(Ba)
Cu	200	131	0.5	<0.14	7.8	57	45	0.4	<0.28	3.1	Ln(Cu+10)‡
Fe	180	82	26.9	<5.6	419.6	52	15	38.0	<7.37	340.3	Ln(Fe+10)‡
Li	34	0	11.1	1.5	30.0	10	6	1.1	<0.56	4.8	Ln(Li)
Mn	218	5	8.5	0.3	159.4	62	1	4.2	0.4	41.0	Ln(Mn)
Ni	185	16	1.3	<0.14	7.3	52	9	0.3	<0.11	1.0	Ln(Ni)
Se	182	98	3.0	<0.11	22.6	52	51	0.2	<0.11	1.0	Ln(Se+1)‡
Sr	149	0	897	67	4342	43	0	82	9	518	Ln(Sr)
U	132	15	0.6	<0.05	2.8	38	38	<MRL	<MRL	<MRL	Ln(U+0.1)
Zn	218	46	21.8	2.2	721.5	62	14	13.3	2.2	69.3	Ln(Zn)

† Trace element means were calculated using ICP/MS read-out estimates as proxy for <MRL values.

‡ Exclude year 2019 (Fe, Se); exclude spring 2019 (Cu).

Major Ion Concentrations:

All major ion concentrations varied positively with SC (Table 4, Figure 4). For the multiple regression models, year was a significant predictor for Cl and Ca; both constituents declined over the 10.5-year study period. Season was a significant predictor for Mg (negative), Na (positive), and K (positive); whereas both season and season x Ln(SC) interaction were significant for SO4 and CO3+HCO3 but with coefficient signs in opposing directions. Calcium, Mg, and SO4 produced models with the greatest precision as indicated by high adjusted R^2 values (nominal comparisons). With this measure, HCO3+CO3 and K exhibited tighter model fits than Na; whereas Cl exhibited the lowest model fit, although still highly significant ($p<0.0001$).

For all of the multiple regression models, Ln(SC) was the predominantly influential variable as indicated by variable importance factors. Hence, the graphical representations of the multiple regression models using only SC as a concentration predictor, with year and season set at mid-range constant values, exhibited close conformance with the mixed-effects model for all seven major ion concentration variables (Figure 4).

Table 4. Models generated for major ion concentrations. Units are mg/L for major ions, µS/cm for specific conductance (SC).

	Multiple Regression			Mixed-Effects	
Y variable / Model terms	**Model Adj. R^2** / Parameter Estimates	p-values: **Model** / Parameter Estimates	Variable Importance, Total Effect†	**Model Adj.R2** / Parameter Estimate	p-value
Ln (SO4)	**0.96**	**<.0001**		**0.96**	
Intercept	-3.39703	<.0001		-3.39738	<.0001
Ln (SC)	1.36861	<.0001	0.986	1.36390	<.0001
Year	0.00597	0.2422	0.0002		
Season	-0.27174	<.0001	0.006		
(Season-0.51613)* (Ln (SC)-5.98919)	0.20526	<.0001			
Ln (CO3+HCO3)	**0.80**	**<.0001**		**0.79**	
Intercept	-0.28704	0.1027		-0.18570	0.1527
Ln (SC)	0.73738	<.0001	0.995	0.75194	<.0001
Year	0.00516	0.4901	0.0005		
Season	0.23242	<.0001	0.013		
(Season-0.51475)* (Ln (SC)-5.97934)	-0.16784	<.0001			
Ln(Cl)	**0.21**	**<.0001**		**0.29**	
Intercept	-0.37683	0.3167		-1.46422	<.0001
Ln (SC)	0.37238	<.0001	0.864	0.38097	<.0001
Year	-0.06899	<.0001	0.132		
Season	0.09094	0.3628	0.003		
Ln (Ca)	**0.98**			**0.98**	
Intercept	-2.55484	<.0001		-2.75169	<.0001
Ln (SC)	1.05831	<.0001	0.983	1.06087	<.0001
Year	-0.01257	0.0001	0.002		
Season	0.03187	0.1138	0.0001		
Ln (Mg)	**0.97**	**<.0001**		**0.97**	
Intercept	-4.36645	<.0001		-4.42580	<.0001
Ln (SC)	1.24272	<.0001	0.998	1.24287	<.0001
Year	-0.00076	0.8565	0.00004		
Season	-0.09098	0.0006	0.0005		
Ln (Na)	**0.62**	**<.0001**		**0.60**	
Intercept	-1.89480	<.0001		-2.07900	<.0001
Ln (SC)	0.71171	<.0001	0.993	0.73157	<.0001
Year	-0.00982	0.3711	0.001		
Season	0.17456	0.0108	0.003		
Ln (K)	**0.82**	**<.0001**		**0.83**	
Intercept	-2.16880	<.0001		-2.26776	<.0001
Ln (SC)	0.54880	<.0001	0.994	0.55200	<.0001
Year	-0.00739	0.1437	0.001		
Season	0.06709	0.0327	0.001		

† Generated with the assumption of independent uniform inputs.

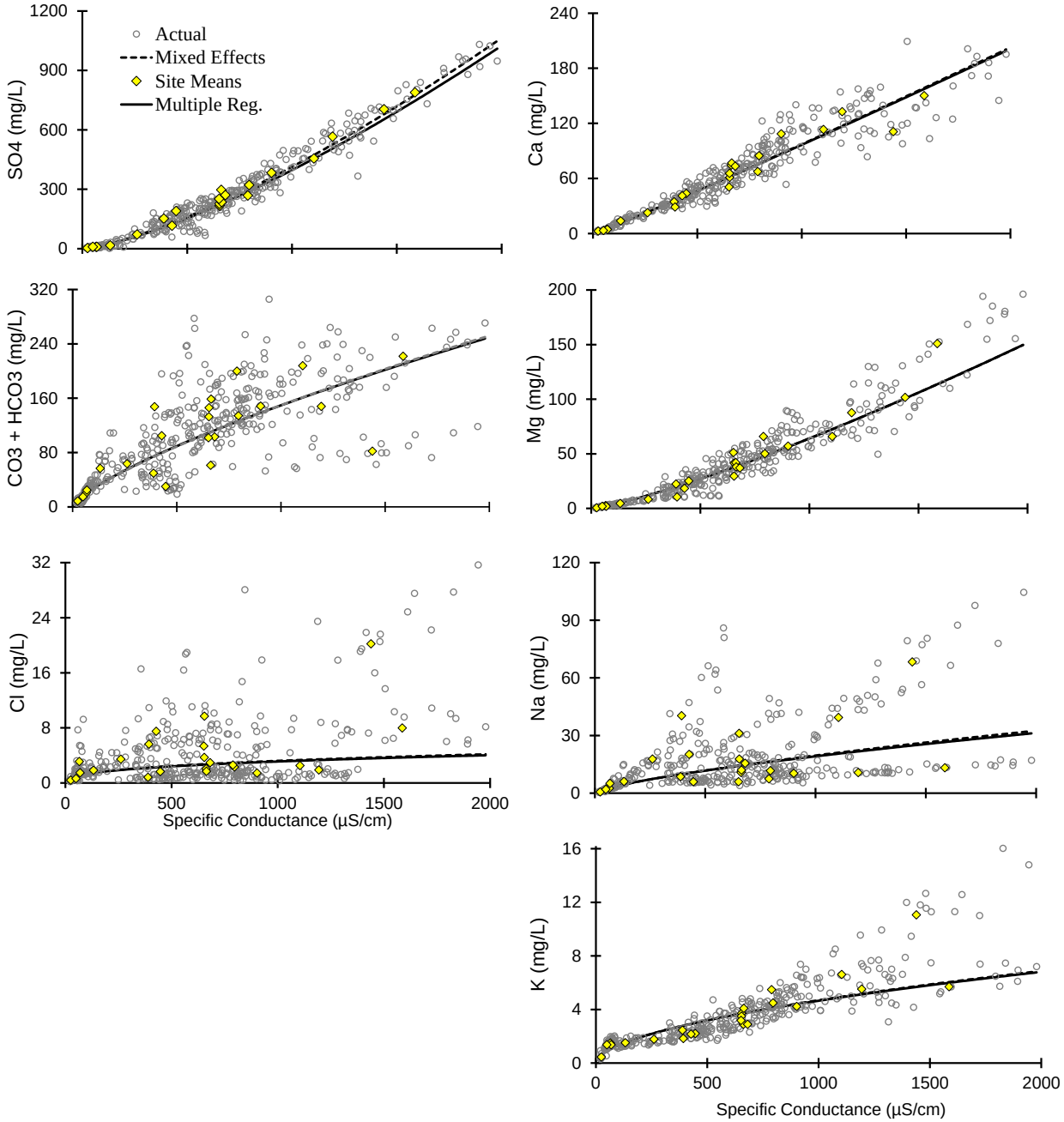

Figure 4. Variation of major ion concentrations with specific conductance for anions (left) and cations (right); measured values (actual), site means, and modeled relationships are denoted. Both models are represented in all charts, although not visible separately in some charts because they are overlaid.

Major Ion Mole Fractions:

For the multiple regression models, year was a significant predictor for the Cl and Mg mole fractions but with only marginal significance for the latter (Table 5). Season was a significant predictor for the two predominant anion mole fractions, CO3+HCO3 and SO4, but with opposing signs. Season was also a significant predictor for two cation mole fractions, Mg and Na, also with opposing signs and with marginal significance for Mg. Six of the seven major-ion mole fractions, all but Ca, exhibited clear and highly significant response to SC (Figure 5). Variable importance factors indicate SC/Ln(SC) to be the predominant influence on all mole fractions except Ca.

Although the Ca mole-fraction model form represented here shows an increasing trend over the SC gradient, the model R^2 value is low and an alternative model form producing residuals with slightly less resemblance to normality [Ln(Ca/Cations) vs. Ln(SC)] produces a p-value>0.05 (data not shown). When plotted against SC (Figure 5), the Ca/Cations variable's rate of change along the SC gradient is of low magnitude relative to those of the other major ions. Hence, the data do not present clear evidence of environmental relevance for the Ca mole-fraction change over the SC gradient.

All multiple regression models for mole fractions have less precision than the corresponding concentration models (Table 4) as indicated by R^2 comparisons. The K and SO4 mole-fraction models exhibit the greatest precision, as indicated by R^2, followed by CO3+HCO3 and Mg. As for the concentration models, the mixed-effects mole-fraction models show close conformance to the multiple regression models with year and season held constant (Figure 5).

In combination, the models represent the various mole fractions with comparative consistency, as the anion mole fractions sum to <5% departure from 1.0 over the entire SC range with the cation fractions sum to <5% departure over most of the SC range (Figure 6). The major-ion matrix composition changes along the SC gradient (Figure 6). As SC increases, the SO4 mole fraction increases at the expense of CO3+HCO3 and Cl, whereas the Mg mole fraction increases at the expense of Na and K.

Table 5. Models generated for major ion mole fractions.

	- - - - - - - - Multiple Regression- - - - - - - -			- - - - Mixed-Effects- - - -	
Y Value/ Model Terms	**Model Adj R^2/** Parameter Estimates	p-values: **Model** / Parameter Estimates	Variable Importance, Total Effect	**Model Adj R^2/** Parameter Estimate	p-values
SO4/Anions	**0.58**	**<.0001**		**0.57**	
Intercept	-0.29405	<.0001		-0.31043	<.0001
Ln (SC)	0.13669	<.0001	0.947	0.13346	<.0001
Year	0.00040	0.8566	0.015		
Season	-0.09100	<.0001	0.058		
(Year-15.6975)* (Ln (SC)-5.98636)	-0.00530	0.0095			
(Season-0.51771)* (Ln (SC)-5.98636)	0.05508	<.0001			
CO3+HCO3/Anions	**0.50**	**<.0001**		**0.48**	
Intercept	1.05938	<.0001		1.12386	<.0001
Ln (SC)	-0.11270	<.0001	0.917	-0.10920	<.0001
Year	0.00264	0.2401	0.003		
Season	0.09503	<.0001	0.104		
(Season-0.51771)* (Ln (SC)-5.98636)	-0.06880	<.0001			
Ln (Cl/Anions)	**0.37**	**<.0001**		**0.44**	
Intercept	0.89872	0.0153		-0.13104	0.6233
Ln (SC)	-0.60877	<.0001	0.938	-0.61085	<.0001
Year	-0.06889	<.0001	0.053		
Season	0.04548	0.6406	0.008		
(Season-0.51771)* (Ln (SC)-5.98636)	0.18001	0.0386			
Ca/Cations	**0.02**	**0.0313**		**0.01**	
Intercept	0.36189	<.0001		0.32933	<.0001
Ln (SC)	0.00818	0.0157	0.787	0.00832	0.0134
Year	-0.00199	0.1081	0.208		
Season	-0.00131	0.8643	0.001		
Mg/Cations	**0.45**	**<.0001**		**0.46**	
Intercept	0.21983	<.0001		0.25082	<.0001
SC	0.00010	<.0001	0.98	0.00010	<.0001
Year	0.00327	0.0313	0.009		
Season	-0.04380	<.0001	0.013		
Ln (Na/Cations)	**0.29**	**<.0001**		**0.26**	
Intercept	-1.18034	<.0001		-1.23321	<.0001
SC	-0.00087	<.0001	0.989	-0.00082	<.0001
Year	-0.00658	0.5036	0.002		
Season	0.16370	0.0079	0.01		
Ln (K/Cations)	**0.77**	**<.0001**		**0.78**	
Intercept	-0.66532	<.0001		-0.66076	<.0001
Ln (SC)	-0.48064	<.0001	0.996	-0.47942	<.0001
Year	-0.00004	0.9943	0.000004		
Season	0.02346	0.4474	0.0003		

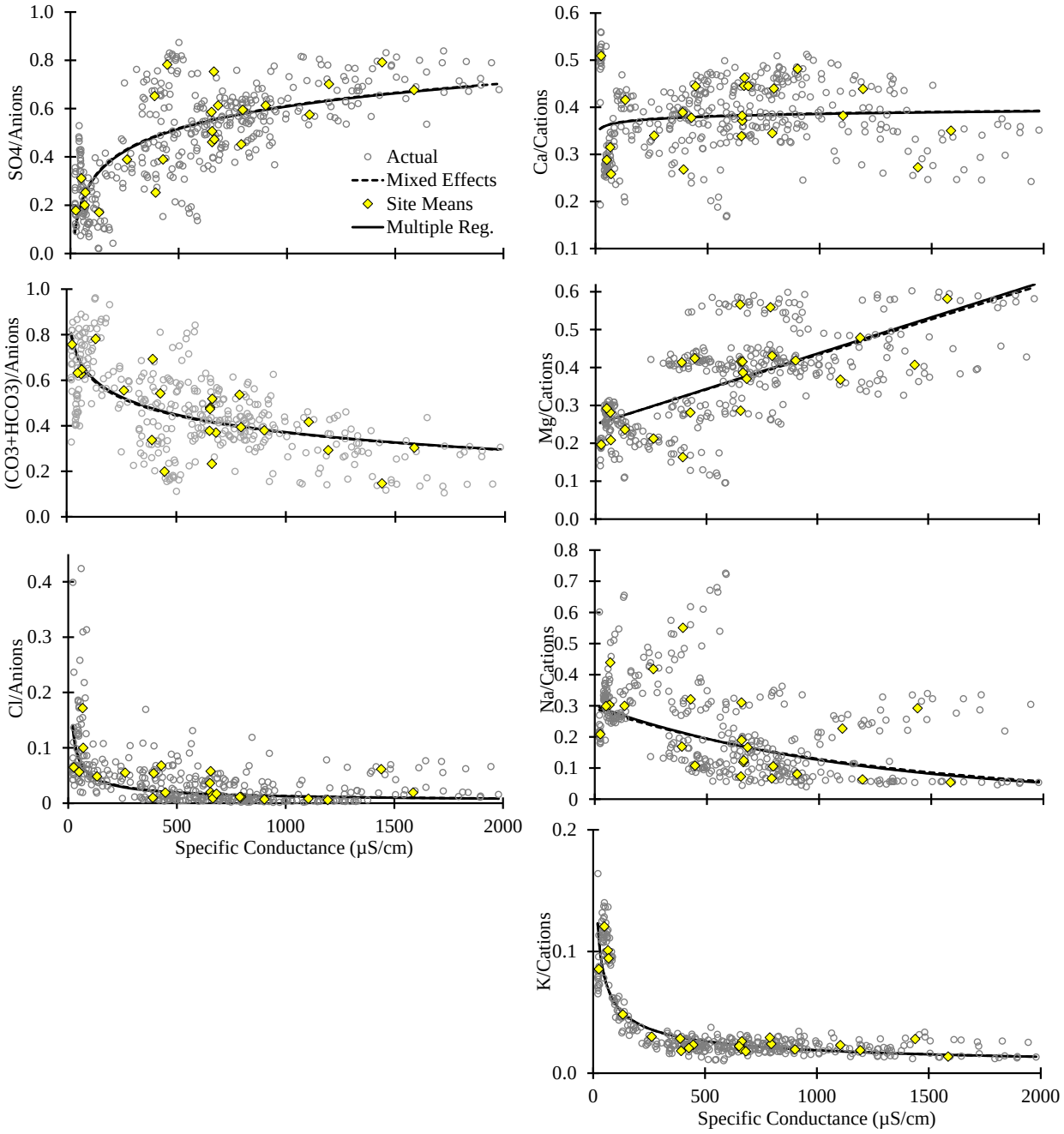

Figure 5. Major ion mole fractions, as measured and as modeled (Table 5). Mixed-effect modeling results are not visible where overlaid by the multiple regression results.

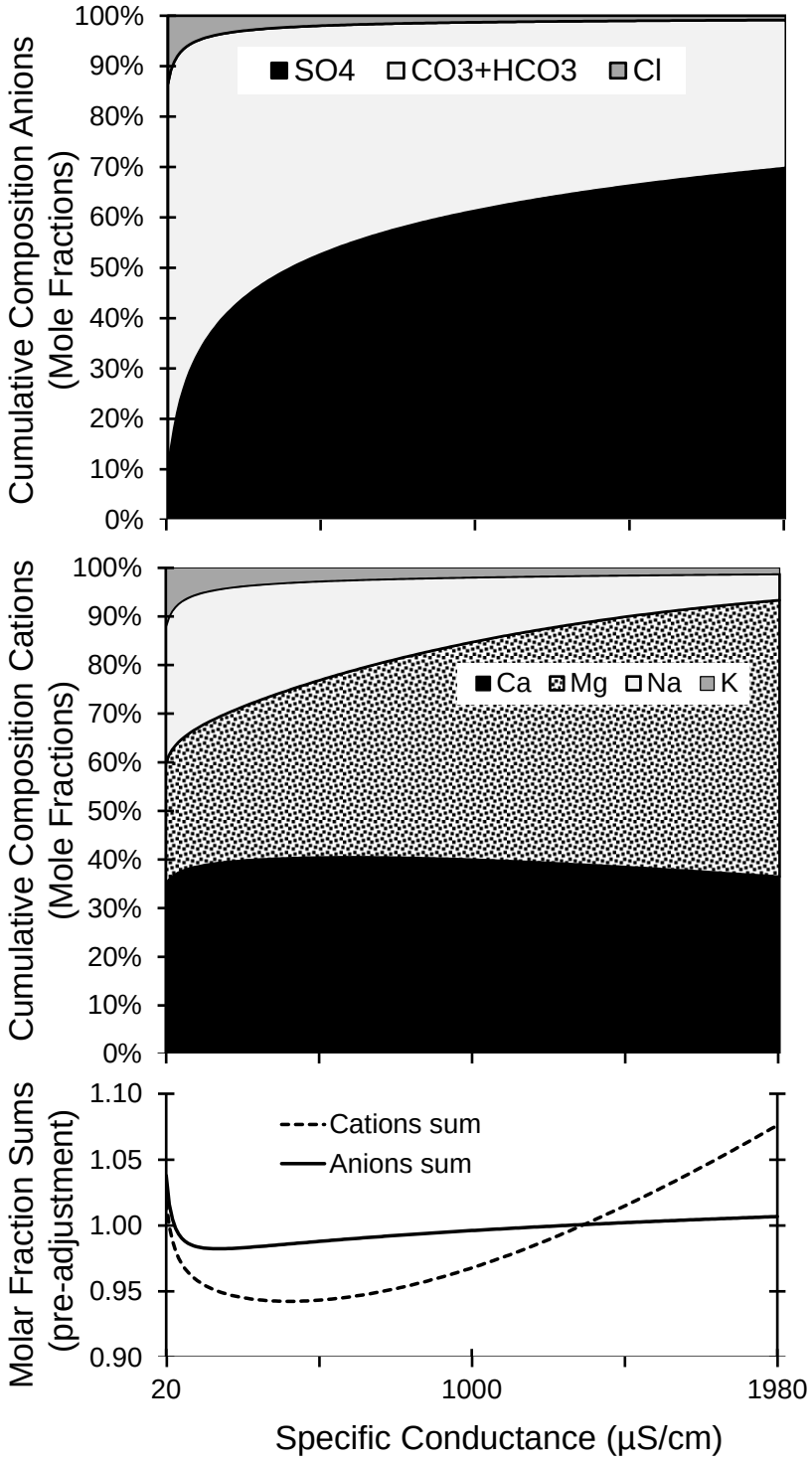

Figure 6. Modeled composition of the major-ion matrix, with proportionate adjustments such sums equal 100%, for anions (upper) and cations (mid); and pre-adjustment molar-fractions sums for cations and anions (lower).

Water pH:

Neither year nor season exhibited significant influence on water pH as independent variables in the multiple regression model, whereas SC exhibited significant influence as did the season x SC interaction (Table 6, Figure 7). Both mixed-effects and multiple regression models demonstrated increasing pH over the SC gradient. A large part of this effect is influenced by reference sites, which have less alkaline waters than the mining-influenced sites. However, running the multiple regression while confining the analysis only to mining-influenced sites produces similar results ($p>0.05$ for year and season but highly significant p-value and positive model coefficient for Ln(SC), although with no significant interaction term, data not shown). As indicated by variable importance factors, Ln(SC) has greater influence on pH than year or season. The mixed-effects model yields a response form that is very similar to that of the multiple regression model with year and pH held constant at mid-range values (Figure 7).

Table 6. Models for pH. Units are standard units for pH, µS/cm for specific conductance (SC).

	Multiple Regression			Mixed-Effects	
Y variable / Model terms	**Model Adj. R^2** / Parameter Estimates	p-values: **Model** / Parameter Estimates	Variable Importance, Total Effect†	**Model Adj.R^2** / Parameter Estimate	p-value
pH	**0.32**			**0.51**	
Intercept	6.71249	<.0001		6.60961	<.0001
Ln (SC)	0.19824	<.0001	0.987	0.20122	<.0001
Year	-0.004195	0.4805	0.002		
Season	0.017659	0.6345	0.026		
(Season-0.51781)* (Ln (SC)-5.968)	-0.094158	0.0035			

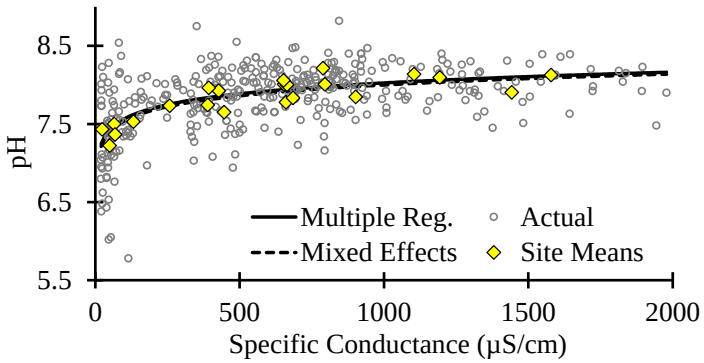

Figure 7. Variation of pH with specific conductance as measured values, as site-mean values, and as modeled (Table 6).

Trace Elements:

Three of the 11 trace elements analyzed (Al, Fe, and Zn) exhibited no significant relationships with SC in either model; whereas a fourth (Cu) exhibited a positive relationship in the mixed effect model but a non-significant relationship ($p<0.05$) in the site-means model (Table 7). Given that Cu is characterized by multiple <MRL observations with nominally negative values and that

the mixed-effects model overestimates statistical significance, the data do not present convincing evidence of consistent response of Cu to the SC gradient (Figure 8). Seven other elements (Ba, Li, Mn, Ni, Se, Sr, and U) exhibit positive responses to SC with p-values <0.05 for both models. Of these, the strongest relationships (as indicated by R^2 values in the site-means model, p-values in both models, and visual analysis of the Figure 8 plots) are exhibited by U, Li, Sr, Ni, and Se in that order.

Table 7. Models generated for trace elements. Units are µg/L for elements, µS/cm for specific conductance (SC).

	- - - - - - - Mixed-Effects - - - - - - - -		- - - - Site Means Model - - - -	
Y variable/ Model terms	**Model Adj. R^2** / Parameter Estimates	p-values	**Model Adj.R^2** / Parameter Estimates	p-values
Ln(Al)	**0.47**		**0.008**	
Intercept	1.76219	<.0001	1.92125	0.0005
Ln (SC)	0.02040	0.4948	0.03059	0.6913
Ln(Ba)	**0.32**		**0.21**	
Intercept	2.33211	<.0001	2.49021	<.0001
Ln (SC)	0.22053	<.0001	0.19555	0.0273
Ln(Cu+10)	**0.68**		**0.12**	
Intercept	2.29221	<.0001	-1.69652	0.0032
Ln (SC)	0.00959	0.0006	0.14047	0.1073
Ln(Fe+10)	**0.17**		**0.002**	
Intercept	3.75299	<.0001	3.27827	0.0017
Ln (SC)	-0.08943	0.0582	-0.02928	0.8463
Ln(Li)	**0.81**		**0.83**	
Intercept	-4.76448	<.0001	-4.90573	<.0001
Ln (SC)	1.09213	<.0001	1.08920	<.0001
Ln(Mn)	**0.14**		**0.17**	
Intercept	-0.59759	0.0703	-0.49158	0.637
Ln (SC)	0.33022	<.0001	0.35038	0.0498
Ln(Ni)	**0.60**		**0.70**	
Intercept	-3.89080	<.0001	-3.61528	<.0001
Ln (SC)	0.59262	<.0001	0.56802	<.0001
Ln(Se+1)	**0.39**		**0.53**	
Intercept	-1.62484	<.0001	-4.93891	<.0001
Ln (SC)	0.40989	<.0001	0.82341	<.0001
Ln(Sr)	**0.60**		**0.76**	
Intercept	-1.09548	<.0001	-1.00645	0.2539
Ln (SC)	1.15353	<.0001	1.14077	<.0001
Ln(U+0.1)	**0.66**		**0.85**	
Intercept	-5.48606	<.0001	-11.24976	<.0001
Ln (SC)	0.73803	<.0001	1.56663	<.0001
Ln(Zn)	**0.49**		**0.12**	
Intercept	2.13283	<.0001	1.97132	0.0012
Ln (SC)	0.05813	0.0657	0.14475	0.109

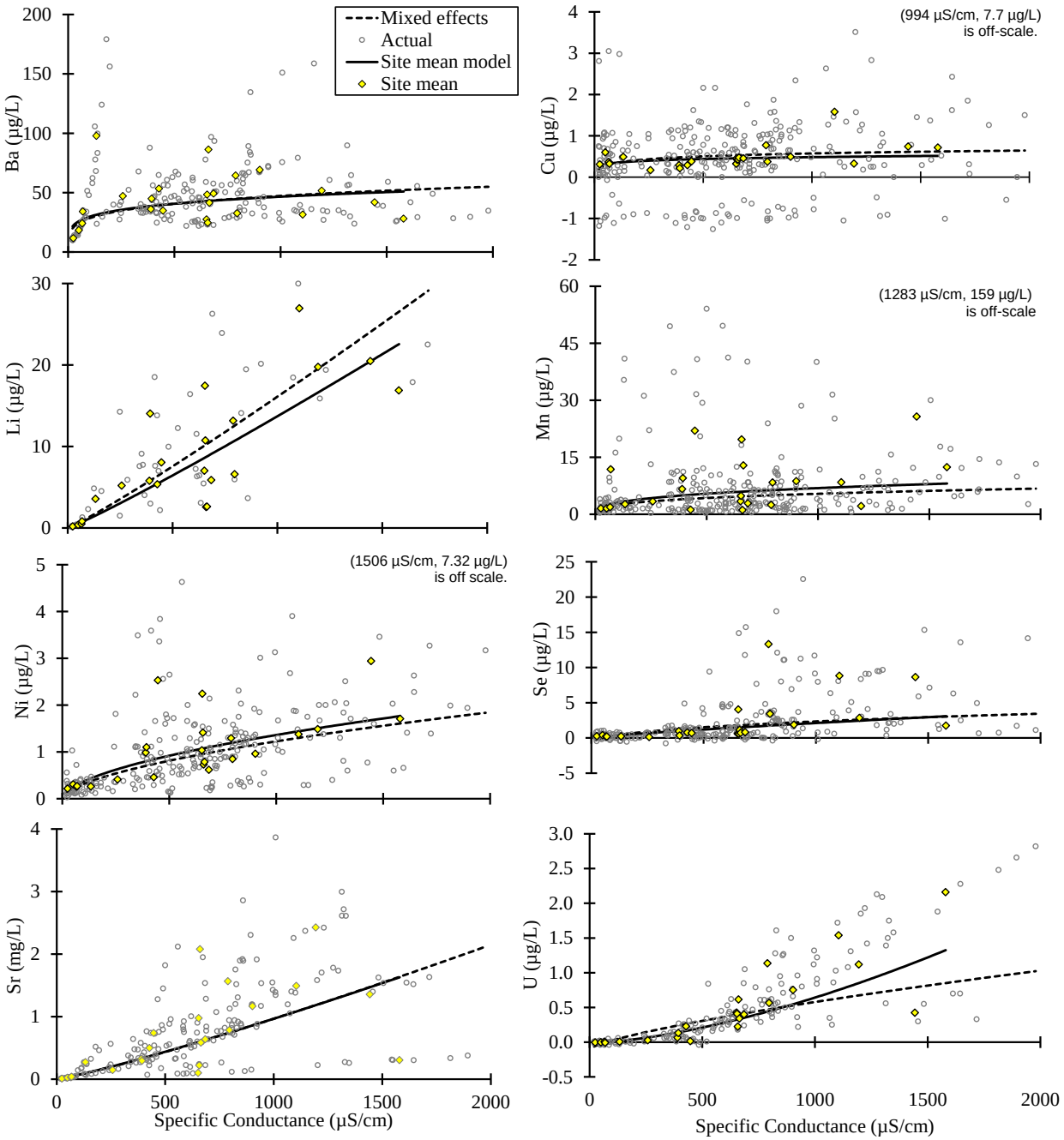

Figure 8. Variation of trace element concentrations with specific conductance as measured values, as site-mean values, and as modeled (Table 7). Only those elements exhibiting nominally significant relationships ($p<0.05$) in one or both models are represented. Data are plotted as instrument read-out values for <MRL observations, as discussed in Methods.

Conclusions

With PRP support, we i) continued monitoring of SC, stage, and flow; ii) conducted seasonal benthic macroinvertebrate and water quality sampling to add to our long-term dataset and enable future long-term recovery assessments; and iii) completed analysis of relationships between SC and ion/trace element concentrations. Contributions of this work include:

- Combining SC and stage data demonstrate general dilution of SC with higher stage (and thus higher flow) and will allow us to account for this flow control in future assessment of stream water chemistry recovery.
- Our data show that all seven major-ion variables predictably vary with SC across 23 central Appalachian streams in two states over 10+ years. Although regressions of all major ions concentrations against SC exhibited positive slopes, some slopes increased more rapidly than others. Hence, our data also show the major-ion matrix varying in a generally predictable pattern across an SC gradient extending up to ~2000 µS/cm, reflecting geochemical mechanisms that occur commonly in Appalachian mine rocks. However, given the lack of significant Year x Ln(SC) interactions for 13 of the 14 major-ion indicators, our data give limited indication of major temporal effects over a decadal time scale. In contrast, most major-ion concentrations and mole fractions (all but Cl and Ca) exhibited significant variation by season. Of particular interest are the offsetting signs of seasonal coefficients for CO3+HCO3 (positive) and SO4 (negative) for both concentrations and mole fractions, given the possibility that HCO3 produced by ecosystem respiration may be influencing water chemistry.
- Certain trace elements also occur at elevated levels in association with elevated SC. Of the eleven trace elements analyzed, five (U, Li, Sr, Ni, and Se) demonstrated that pattern with the greatest consistency. Of these five, only Se was found to exceed regulatory criteria intended to protect aquatic life (3.1 µg/L; US EPA 2021); but we note that there remain unknowns regarding ecotoxicological effects of elevated trace elements in high-SC Appalachian mine waters.
- We have conducted two rounds of streamflow measurements at our six selected streams, and thus more flow measurements are needed to develop rating curves between flow and stage. We emphasize, however, that this PRP support has allowed us to install stage recorders, to initiate flow measurement methods, and to develop SC-concentration relationships; these resources will be leveraged along with match student support to continue data collection and flow measurements. Once rating curves are completed, the student as the focus of their MS thesis will use data and developed models for novel estimates of downstream mass export.
- Data and methods generated through this PRP project will support a resubmission of our proposal to the National Science Foundation to understand potential water chemistry effects to stream carbon cycling. Specifically, proposed work will rely on flow-stage rating curves (for carbon export estimates) and SC-concentration relationships (to assess covarying water quality stressors). We plan to submit this proposal in fall 2021.

Literature Cited

Battin, T.J., Luyssaert, S., Kaplan, L.A., Aufdenkampe, A.K., Richter, A. and Tranvik, L.J. 2009. The boundless carbon cycle. *Nature Geoscience*, *2*(9), p.598.

Boehme, E.A., Zipper, C.E., Schoenholtz, S.H., Soucek, D.J., & Timpano, A.J. 2016. Temporal dynamics of benthic macroinvertebrate communities and their response to elevated specific conductance in Appalachian coalfield headwater streams. *Ecological Indicators*, *64*, 171-180.

Cianciolo, T. R., McLaughlin, D. L., Zipper, C. E., Timpano, A. J., Soucek, D. J., & Schoenholtz, S. H., 2020a. Impacts to water quality and biota persist in mining-influenced Appalachian streams. *Science of the Total Environment*. https://doi.org/10.1016/j.scitotenv.2020.137216

Cianciolo T.R., D.L. McLaughlin, C.E. Zipper, A.J. Timpano, D.J. Soucek, K.M. Whitmore, S.H. Schoenholtz. 2020b. Selenium bioaccumulation across trophic levels and along a longitudinal gradient in headwater streams. *Environmental Toxicology and Chemistry*. https://setac.onlinelibrary.wiley.com/doi/abs/10.1002/etc.4660

Clark E.V., B.M. Greer, C.E. Zipper, E.T. Hester. 2016. Specific conductance-stage relationships in Appalachian valley fill streams. Environmental Earth Sciences 75:1222.

Drover, D.R. 2018. Benthic macroinvertebrate community structure responses to multiple stressors in mining-influenced streams of central Appalachia USA. (Doctoral dissertation, Virginia Tech).

Gomi, T., Sidle, R.C., & Richardson, J.S. 2002. Understanding processes and downstream linkages of headwater systems: headwaters differ from downstream reaches by their close coupling to hillslope processes, more temporal and spatial variation, and their need for different means of protection from land use. *BioScience*, *52*(10), 905-916.

Griffith, M.B., Norton, S.B., Alexander, L.C., Pollard, A.I., & LeDuc, S.D. 2012. The effects of mountaintop mines and valley fills on the physicochemical quality of stream ecosystems in the central Appalachians: a review. *Science of the Total Environment*, *417*, 1-12.

Hartman, K.J., Kaller, M.D., Howell, J.W., & Sweka, J.A. 2005. How much do valley fills influence headwater streams?. *Hydrobiologia*, *532*(1-3), 91.

Hirsch, R.M., Slack, J.R., & Smith, R.A. 1982. Techniques of trend analysis for monthly water quality data. *Water resources research*, *18*(1), 107-121.

Johnson, B., Smith, E., Ackerman, J.W., Dye, S., Polinsky, R., Somerville, E., Decker, C., Little, D., Pond, G.J. and D'Amico, E. 2019. Spatial Convergence in Major Dissolved Ion Concentrations and Implications of Headwater Mining for Downstream Water

Quality. *JAWRA Journal of the American Water Resources Association*, *55*(1), pp.247-258.

Leopold, L.B., Wolman, M.G., & Miller, J.P. 1964. Channel form and process. Fluvial processes in geomorphology. San Francisco, CA: WH Freeman and company, 198-322.

Moore, R.D. 2005. Slug injection using salt in solution. *Streamline Watershed Management Bulletin*. vol. 8, no. 2, 2005, pp. 1-6.

Pence, R.A. 2019. Comparison of Quantitative and Semi-Quantitative Assessments of Benthic Macroinvertebrate Community Response to Elevated Salinity in central Appalachian Coalfield Streams. (M.S. thesis, Virginia Tech).

Pond, G.J., Passmore, M.E., Borsuk, F.A., Reynolds, L., & Rose, C. J. 2008. Downstream effects of mountaintop coal mining: comparing biological conditions using family-and genus-level macroinvertebrate bioassessment tools. *Journal of the North American Benthological Society*, *27*(3), 717-737.

Sams, J.I., & Beer, K.M. 2000. Effects of coal-mine drainage on stream water quality in the Allegheny and Monongahela River basins—Sulfate transport and trends. *Water Resources Investigations Report*, 99-4208.

Timpano, A.J., Schoenholtz, S.H., Soucek, D.J., & Zipper, C.E. 2015. Salinity as a limiting factor for biological condition in Mining-Influenced central Appalachian headwater streams. *Journal of the American Water Resources Association*, *51*(1), 240-250.

Timpano, A.J., Schoenholtz, S.H., Soucek, D.J., & Zipper, C.E. 2018. Benthic macroinvertebrate community response to salinization in headwater streams in Appalachia USA over multiple years. *Ecological Indicators*, *91*, 645-656.

Vander Vorste, R., Timpano, A.J., Cappellin, C., Badgley, B.D., Zipper, C.E., & Schoenholtz, S.H. 2019. Microbial and macroinvertebrate communities, but not leaf decomposition, change along a mining-induced salinity gradient. *Freshwater Biology*, *64*(4), 671-684.

Whitmore, K.M., Schoenholtz, S.H., Soucek, D.J., Hopkins, W.A., & Zipper, C.E. 2018. Selenium dynamics in headwater streams of the central Appalachian coalfield. *Environmental Toxicology and Chemistry*, *37*(10), 2714-2726.

Whitmore K.M.; S.H. Schoenholtz; D.J. Soucek; C.E. Zipper (2021): Trace Element Bioaccumulation in Appalachian Coalfield Streams. University Libraries, Virginia Tech. Dataset. https://doi.org/10.7294/qrkk-qk46